



# Impact of *APOE* $\epsilon$ 4 Carrier Status on Associations Between Subthreshold, Positive Amyloid- $\beta$ Deposition, Brain Function, and Cognitive Performance in Cognitively Normal Older Adults: A Prospective Study

Dong Woo Kang<sup>1</sup>, Sheng-Min Wang<sup>2</sup>, Yoo Hyun Um<sup>3</sup>, Nak-Young Kim<sup>4</sup>, Chang Uk Lee<sup>1</sup> and Hyun Kook Lim<sup>2\*</sup>

<sup>1</sup> Department of Psychiatry, Seoul St. Mary's Hospital, College of Medicine, The Catholic University of Korea, Seoul, South Korea, <sup>2</sup> Department of Psychiatry, Yeouido St. Mary's Hospital, College of Medicine, The Catholic University of Korea, Seoul, South Korea, <sup>3</sup> Department of Psychiatry, St. Vincent's Hospital, College of Medicine, The Catholic University of Korea, Seoul, South Korea, <sup>4</sup> Department of Psychiatry, Keyo Hospital, Uiwang, South Korea

## OPEN ACCESS

### Edited by:

Boon-Seng Wong,  
Singapore Institute of  
Technology, Singapore

### Reviewed by:

Hwamee Oh,  
Brown University, United States  
Karin Meeker,  
Washington University in St. Louis,  
United States

### \*Correspondence:

Hyun Kook Lim  
drblues@catholic.ac.kr

### Specialty section:

This article was submitted to  
Alzheimer's Disease and Related  
Dementias,  
a section of the journal  
Frontiers in Aging Neuroscience

**Received:** 08 February 2022

**Accepted:** 12 April 2022

**Published:** 23 May 2022

### Citation:

Kang DW, Wang S-M, Um YH,  
Kim N-Y, Lee CU and Lim HK (2022)  
Impact of *APOE*  $\epsilon$ 4 Carrier Status on  
Associations Between Subthreshold,  
Positive Amyloid- $\beta$  Deposition, Brain  
Function, and Cognitive Performance  
in Cognitively Normal Older Adults: A  
Prospective Study.  
*Front. Aging Neurosci.* 14:871323.  
doi: 10.3389/fnagi.2022.871323

**Background:** A growing body of evidence suggests a deteriorating effect of subthreshold amyloid-beta ( $A\beta$ ) accumulation on cognition before the onset of clinical symptoms of Alzheimer's disease (AD). Despite the association between the  $A\beta$ -dependent pathway and the *APOE*  $\epsilon$ 4 allele, the impact of this allele on the progression from the subthreshold  $A\beta$  deposits to cognitive function impairment is unclear. Furthermore, the comparative analysis of positive  $A\beta$  accumulation in the preclinical phase is lacking.

**Objective:** This study aimed to explore the differential effect of the *APOE*  $\epsilon$ 4 carrier status on the association between  $A\beta$  deposition, resting-state brain function, and cognitive performance in cognitively normal (CN) older adults, depending on the  $A\beta$  burden status.

**Methods:** One hundred and eighty-two older CN adults underwent resting-state functional magnetic resonance imaging, [<sup>18</sup>F] flutemetamol (FMM) positron emission tomography, a neuropsychological battery, and *APOE* genotyping. We evaluated the resting-state brain function by measuring the local and remote functional connectivity (FC) and measured the remote FC in the default-mode network (DMN), central-executive network (CEN), and salience network (SN). In addition, the subjects were dichotomized into those with subthreshold and positive  $A\beta$  deposits using a neocortical standardized uptake value ratio with the cut-off value of 0.62, which was calculated with respect to the pons.

**Results:** The present result showed that *APOE*  $\epsilon$ 4 carrier status moderated the relationship between  $A\beta$  deposition, local and remote resting-state brain function, and cognitive performance in each CN subthreshold and positive  $A\beta$  group. We observed the following: (i) the *APOE*  $\epsilon$ 4 carrier status- $A\beta$  deposition and *APOE*  $\epsilon$ 4 carrier status-local FC interaction for the executive and memory function; (ii) the *APOE*  $\epsilon$ 4 carrier

status-regional A $\beta$  accumulation interaction for the local FC; and (iv) the *APOE*  $\epsilon$ 4 carrier status-local FC interaction for the remote inter-network FC between the DMN and CEN, contributing higher cognitive performance in the *APOE*  $\epsilon$ 4 carrier with higher inter-network FC. Finally, these results were modulated according to A $\beta$  positivity.

**Conclusion:** This study is the first attempt to thoroughly examine the influence of the *APOE*  $\epsilon$ 4 carrier status from the subthreshold to positive A $\beta$  accumulation during the preclinical phase.

**Keywords:** *APOE*  $\epsilon$ 4 allele, subthreshold amyloid-beta, regional homogeneity, functional connectivity, cognitively normal older adults

## INTRODUCTION

Amyloid- $\beta$  (A $\beta$ ) accumulation differentiates Alzheimer's disease (AD) from other neurodegenerative diseases (Jack et al., 2018). Additionally, the A $\beta$  deposition has been known to progress non-linearly in decades before the onset of clinical symptoms of AD (Jack et al., 2013). In this regard, the preclinical stage of AD has therefore been defined as the presence of A $\beta$  pathology without signs of significant cognitive impairment due to AD dementia (Knopman et al., 2012). In addition, the period before AD symptoms, which has become apparent, also attracts clinical attention as the right time for primary intervention because the A $\beta$ -dependent pathophysiology is not yet fully advanced. Although this period could be overlooked in the clinical field due to the lack of apparent clinical symptoms, preclinical AD participants have demonstrated an increased risk of transition to MCI and AD (Knopman et al., 2012), as well as the deteriorating effects on the cognitive performance, brain structure, and function (Hedden et al., 2009; Mattsson et al., 2014; Baker et al., 2017).

Amyloid- $\beta$  deposition is evaluated using A $\beta$ -positron emission tomography (PET) for the early detection of preclinical AD and there has been renewed interest in A $\beta$  accumulation below the threshold for a positive scan (Bischof and Jacobs, 2019). Even among individuals with a negative PET scan, 65% showed an early autopsy stage of A $\beta$  accumulation (Thal phase 2), and 15% displayed an advanced stage (Thal phase 4 or 5) (Salloway et al., 2017). Additionally, specific brain regions, including the orbitofrontal cortex, the anterior cingulate cortex, and the precuneus, are prone to the earliest A $\beta$  accumulation compared with other brain regions (Sojkova et al., 2011; Driscoll et al., 2012; Villeneuve et al., 2015). In addition, the regional A $\beta$  deposits predicted cognitive decline more accurately than global deposition in cognitively normal (CN) older adults with subthreshold A $\beta$  accumulation (Farrell et al., 2018). Moreover, the subthreshold A $\beta$  deposits were associated with functional impairment (Insel et al., 2017), brain atrophy (Mattsson et al., 2014), and dysfunction of the brain functional networks (Palmqvist et al., 2017), and predicted further A $\beta$  and tau deposition (Leal et al., 2018; Farrell et al., 2021).

*APOE*  $\epsilon$ 4 allele has been demonstrated to modulate the penetrance and weight of A $\beta$  pathophysiological cascade (Frisoni et al., 2022) and to account for the largest proportion of the genetic risk factors for sporadic AD (Sims et al., 2020). In this

regard, the *APOE*  $\epsilon$ 4 allele has been known to increase the risk of sporadic AD occurrence in a dose-dependent manner (Corder et al., 1993). The *APOE*  $\epsilon$ 4 allele has also been reported to increase A $\beta$  production (DeMattos et al., 2004), reduce the clearance of A $\beta$  (Castellano et al., 2011), and affect tau binding (Small et al., 2009). Lastly, *APOE*  $\epsilon$ 4 fragments have been demonstrated to interact synergistically with AD pathology, deteriorating the degree of neurodegeneration (Andrews-Zwilling et al., 2010; Bien-Ly et al., 2011). Therefore, the progression of sporadic AD cannot be fully understood without the consideration of the *APOE* genotype.

In addition, the changes in brain function have been demonstrated to precede those in the brain structure and track pathophysiological processes in the preclinical phase (Jack et al., 2013). Among the various methodologies employed for evaluating brain function, functional connectivity (FC) is a widely used and reliable method for evaluating functional interactions in the brain connectome (Biswal et al., 2010). In addition, the earliest accumulation of A $\beta$  is known to affect FC (Palmqvist et al., 2017), and existing research has recognized the impact of the *APOE*  $\epsilon$ 4 allele on brain function and cognitive performance in the preclinical phase of AD. Previous research has found disrupted FC from the precuneus in the *APOE*  $\epsilon$ 4 carrier of the CN without positive A $\beta$  deposition (Sheline et al., 2010). In another study, the authors demonstrated an altered within-network FC in the *APOE*  $\epsilon$ 4 carrier of the CN (Wu et al., 2016). Recently, investigators have reported a simultaneous structural and functional disruption that mediates memory impairment in the CN with the *APOE*  $\epsilon$ 4 allele (Li et al., 2021). However, the generalizability of this previous research is limited because most of these studies lacked information on A $\beta$  deposition; they only evaluated the remote FC of predefined brain regions and showed results with weak statistical significance.

While a static FC is based on the assumed temporal stationarity of functional networks, the dynamic FC considers the dynamic nature of brain activity in faster timescales by selecting a time window that is shifted in time by a fixed number of data points (Hutchison et al., 2013). This dynamic FC has shown a significant association with the subthreshold A $\beta$  accumulation in the preclinical phase; however, the interaction with the *APOE*  $\epsilon$ 4 allele was not evaluated in this prior study (Hahn et al., 2019). Moreover, results from dynamic FC must be interpreted with caution due to the arbitrariness of dynamic FC parameters and its vulnerability to physiological noise that could drive dynamic states (Laumann et al., 2017). These factors contribute to weaker

reliability and reproducibility of dynamic FC than a static FC (Abrol et al., 2017).

Together, these studies provide important insights into the subthreshold A $\beta$ , the pivotal role of the *APOE*  $\epsilon$ 4 allele, and the FC biomarker in the trajectory of AD. However, there remains a paucity of comprehensive evidence on the impact of *APOE* genotype on associations between subthreshold, positive A $\beta$  accumulation, brain function, and cognitive performance in the preclinical phase of AD.

In this regard, the current study classified the CN group according to the presence of the *APOE*  $\epsilon$ 4 allele in each CN group with subthreshold A $\beta$  deposition (CN sub-A $\beta$ ) and those with positive deposition (CN A $\beta$ +). We aimed to evaluate the differential impact of the *APOE*  $\epsilon$ 4 carrier status on the association between the subthreshold, positive A $\beta$  accumulation, FC, and cognitive performance in the preclinical phase. Additionally, local and remote FC evaluation of functional synchronization at different spatial scales in the brain connectome (Sepulcre et al., 2010) has been suggested to enhance network information capacity and discrimination accuracy of the global network (Deco et al., 2014). In this regard, the local-to-remote FC has been suggested to provide a comprehensive understanding of AD (Liu et al., 2014; Li et al., 2021). Therefore, the present study assessed the effect of the *APOE*  $\epsilon$ 4 carrier status by measuring the local and remote FC in an integrative manner. Furthermore, we included information on both global and regional A $\beta$  accumulation and evaluated both memory performance and executive functions being affected at an initial stage for detecting subtle differences in A $\beta$  burden and cognitive function in the earliest course of AD (Buckner, 2004; Farrell et al., 2018). In addition, we hypothesized that the *APOE*  $\epsilon$ 4 carrier would show a distinct pathway from A $\beta$  deposition to cognitive function *via* differences in the local and remote FC in each CN sub-A $\beta$  and A $\beta$ + group.

## MATERIALS AND METHODS

### Participants

A total of 182 CN, consisting of 110 with subthreshold A $\beta$  deposition [CN sub-A $\beta$  group (age range: 55–80 years), 30 subjects in the *APOE*  $\epsilon$ 4 carrier, 80 subjects in the *APOE*  $\epsilon$ 4 non-carrier], 72 with positive A $\beta$  deposition [CN A $\beta$ + group (age range: 57–84 years), 34 subjects in the *APOE*  $\epsilon$ 4 carrier, and 38 subjects in the *APOE*  $\epsilon$ 4 non-carrier], were included in the study. Subjects were recruited from volunteers of the Catholic Aging Brain Imaging database, which contains brain scans of patients who visited the outpatient clinic at the Catholic Brain Health Center, Yeouido St. Mary's Hospital, the Catholic University of Korea, from 2017 to 2021.

### Neuropsychological Assessment

The cognitive function of all subjects was assessed using the Korean version of the Consortium to Establish a Registry for AD (CERAD-K) (Lee et al., 2002). Measurements included assessment in the Korean version of the verbal fluency (VF) test, the 15-item Boston naming test, mini-mental state examination (MMSE-K) (Park, 1989), word list memory (WLM), word list

recall (WLR), word list recognition (WLRc), constructional praxis, and constructional recall. In addition, total memory (TM) domain scores were obtained by summing up the scores from the WLM, WLR, and WLRc. The total CERAD-K scores were calculated by summing up all subcategory scores, excluding the MMSE-K score. Additionally, the Stroop Word-Color Interference Test and the Trail Making Test B were used to assess executive functioning (Stroop, 1935; Tombaugh, 2004), along with the VF. Higher Trail Making Test B scores mean lower executive function. Details regarding the usage of specific tests and the reviewing process are described in the **Supplementary Material**. The inclusion criteria were as follows: (1) unimpaired memory function, quantified by scoring above age-, sex-, and education-adjusted cut-offs on the WLM, WLR, and WLRc domains, (2) MMSE-K score between 24 and 30, (3) Clinical Dementia Rating score of 0, (4) Memory Box score of 0, (5) normal cognitive function based on the absence of significant impairment in cognitive functions or activities of daily living, and (6) participants without a family history of AD. We excluded participants with a history of alcoholism, drug abuse, head trauma, or psychiatric disorders, those taking any psychotropic medications (e.g., cholinesterase inhibitors, antidepressants, benzodiazepines, and antipsychotics), those with multiple vascular risk factors, and those with extensive cerebrovascular disease. T2-weighted fluid-attenuated inversion recovery data were acquired to objectively exclude vascular lesions or other diseases. Participants underwent [ $^{18}$ F] flutemetamol (FMM) PET-CT within 3 months before or after the magnetic resonance imaging (MRI) scan. The procedures for *APOE* genotyping are described in the **Supplementary Material**. We excluded participants with the *APOE*  $\epsilon$ 2 allele. If the participants had at least one *APOE*  $\epsilon$ 4 allele, they were categorized as *APOE*  $\epsilon$ 4 carriers; if they had no *APOE*  $\epsilon$ 4 allele, they were categorized as *APOE*  $\epsilon$ 4 non-carriers. The study was conducted under the ethical and safety guidelines set forth by the Institutional Review Board of the Catholic University of Korea, which approved all research activities. Informed written consent was obtained from all the participants.

### Functional MRI Data Processing

Detailed procedures for structural and functional MRI (fMRI) data acquisition are described in the **Supplementary Material**. We used the Data Processing Assistant for resting-state fMRI (rfMRI) (DPARFSE, GNU General Public License, Beijing, China) (Yan and Zang, 2010), which is based on the Statistical Parametric Mapping (SPM 12, <http://www.fil.ion.ucl.ac.uk/spm>, Wellcome Centre for Human Neuroimaging, London, England), to preprocess the fMRI images. The preprocessing included slice timing, realignment for motion corrections, spatial registration, normalization, and smoothing. This procedure is demonstrated in detail in our previous study (Kang et al., 2021) and in the **Supplementary Material**.

### Local Functional Connectivity Analysis: Regional Homogeneity

Local FC is defined by the temporal coherence or synchronization of the BOLD time series within a set of nearest neighbors

of a given voxel. Regional homogeneity (ReHo) is the most representative and reliable index of the local FC (Jiang and Zuo, 2016). The ReHo maps of all participants were made using a general routine using the DPARSF. Briefly, we set the basic cube to calculate Kendall's coefficient of concordance (KCC) by  $3 \text{ mm} \times 3 \text{ mm} \times 3 \text{ mm}$  voxels. The KCC is obtained from Kendall's rank correlation (Kendall and Gibbons, 1990) and it measures the similarity of the time series of a given voxel to those of its nearest neighbors in a voxel-wise way (Zang et al., 2004). Therefore, the KCC value of the central voxel in the cube was calculated by referring to the temporal sequences of the neighboring 26 voxels. The calculated value was assigned as the ReHo value of the central voxel. To improve the comparability between subjects, standard normal z-transformation was applied to all ReHo maps (zReHo maps). Finally, these "zReHo maps" were spatially smoothed using a 6 mm full width at half maximum Gaussian kernel for the following statistical analysis.

### Remote Functional Connectivity Analysis: Intra- and Inter-Network Connectivity

Regarding the remote FC, we used the default-mode network (DMN) (Sorg et al., 2007; Zhu et al., 2013), central-executive network (CEN) (Weiler et al., 2014), and salience network (SN) (He et al., 2014) that have been demonstrated to be selectively disrupted in the trajectory of AD. In addition, intra- and inter-networks FC of these resting-state networks have been reported to be affected by AD progression (Brier et al., 2012; Wang et al., 2015). Twenty-one spherical (6 mm radius) regions of interest (ROIs) that represented the DMN, CEN, and SN have been described in a previous study (Brier et al., 2012); the Montreal Neurological Institute coordinates of these 21 ROIs are presented in **Supplementary Table S1**. The representative mean time series were estimated by averaging the time series of all voxels in the ROI. Pearson's correlation coefficients were computed between each pair of ROIs for each subject. Fisher's r-to-z transformation was applied to obtain Z-scores and to improve the normality of the correlation coefficients. For each of the three resting-state networks, the intra-network strength was defined as the mean connection strength of the ROIs in the same network (**Supplementary Material**). In each pair of networks, the strength of the inter-network connectivity was defined as the mean strength of all possible connections (**Supplementary Material**).

### [<sup>18</sup>F]-Flutemetamol PET Image Acquisition and Processing

[<sup>18</sup>F] flutemetamol was manufactured, and FMM-PET data were collected and analyzed as described previously (Thurfjell et al., 2014). The MRI of each participant was used to co-register and define the ROIs and correct partial volume effects arising from the expansion of cerebrospinal spaces accompanying the cerebral atrophy. Static PET scans were acquired from 90 to 110 min after 185 MBq of FMM injection. The semi-quantification of FMM uptake on PET/CT scan was performed by obtaining the standardized uptake value ratios (SUVRs). The volumes of interest (VOIs) were restricted to gray matter, covering

the frontal, superior parietal, lateral temporal, anterior, and posterior cingulate cortex/precuneus regions. These VOIs were also considered in a previous study (Thurfjell et al., 2014). The reference region for SUVR calculations was pons. The mean uptake counts of each VOIs and reference region were measured on the preprocessed image. A regional SUVR was calculated as the ratio of each cortical regional mean count to the pons mean count (SUVR<sub>PONS</sub>). The global cortical average (composite SUVR) was calculated by averaging the regional cortical SUVRs weighted for size. We used a cut-off for "positive" or "subthreshold" neocortical SUVR of 0.62, consistent with the cut-off values used in a previous FMM PET study (Thurfjell et al., 2014). PET scans classified as subthreshold A $\beta$  accumulation also exhibited normal visual reading. Detailed information on the PET scan and SUVR calculation are provided in the **Supplementary Material**.

### Statistical Analysis

Statistical analyses were performed using R software (version 2.15.3), jamovi (version 1.6.23) (<https://www.jamovi.org>), and SPM 12. Assumptions of normality were tested for continuous variables using the Kolmogorov–Smirnov test in R software; all data demonstrated a normal distribution. The two-sample *t*-test and chi-squared ( $\chi^2$ ) tests were used to probe for differences in demographic variables, clinical data, regional and global A $\beta$  deposition, and cognitive function between APOE  $\epsilon$ 4 carriers and non-carriers in each CN sub-A $\beta$  and A $\beta$ + group, respectively. All statistical analyses used a two-tailed *P*-value < 0.05 to define statistical significance.

A multiple regression analysis was applied to investigate the effects of APOE  $\epsilon$ 4 carrier status-by-A $\beta$  accumulation interactions on the neuropsychological test scores in each CN sub-A $\beta$  and A $\beta$ + group. CERAD-K subdomain, TM, and total CERAD-K scores were the dependent variables, while APOE  $\epsilon$ 4 carrier status, regional, and global FMM SUVR<sub>PONS</sub> were the independent variables. Age, sex, and years of education were included as covariates. We applied a threshold of  $\alpha = 0.05$  to consider significant regression weights, and we additionally accounted for multiple testing using the Bonferroni correction for each hypothesis (multiplying the *P*-value by a factor of 12 subdomains of the CERAD-K battery). In addition, each variable was z-transformed using the mean and standard deviation for further analysis.

To compare the difference in the local FC depending on the APOE  $\epsilon$ 4 carrier status, ANCOVA on a voxel-by-voxel basis was carried out between the APOE  $\epsilon$ 4 carriers and non-carriers on the individual z maps of ReHo in each CN sub-A $\beta$  and A $\beta$ + group. Age, sex, and years of education were included as covariates in the statistical tests. We designed an ANCOVA based on SPM 12. All statistical maps were corrected for multiple comparisons using Gaussian random field (GRF) correction combining the voxel *P*-value < 0.001 and cluster level < 0.05 in DPABI\_V5.1\_201201 (<http://rfmri.org/dpabi>, GNU GENERAL PUBLIC LICENSE, Beijing, China) (Bansal and Peterson, 2018). This cluster-wise method based on the random field theory is recommended for multiple comparisons of ReHo (Jiang and Zuo, 2016). In addition, zReHo values from brain

**TABLE 1 |** Demographic and clinical characteristics of study participants.

<b>(A) Cognitively normal older adults with subthreshold A<math>\beta</math> deposition.</b>			
<i>APOE</i> $\epsilon$ 4 carrier status	<b>Non-carrier</b>	<b>Carrier</b>	<b><i>P</i>-value</b>
	<b>(<i>n</i> = 80)</b>	<b>(<i>n</i> = 30)</b>	
Age	67.0 $\pm$ 6.1	67.3 $\pm$ 7.7	0.850
Gender			
Male	23 (28.8%)	10 (33.3%)	
Female	57 (71.2%)	20 (66.7%)	
Education years	12.8 $\pm$ 3.6	12.7 $\pm$ 4.1	0.951
Global SUVR <sub>PONS</sub>	0.56 $\pm$ 0.03	0.55 $\pm$ 0.04	0.204
<b>Regional SUVR<sub>PONS</sub></b>			
ACC	0.57 $\pm$ 0.04	0.58 $\pm$ 0.05	0.323
FL	0.44 $\pm$ 0.04	0.43 $\pm$ 0.04	0.230
PL	0.37 $\pm$ 0.04	0.38 $\pm$ 0.06	0.563
PCC/precuneus	0.49 $\pm$ 0.04	0.48 $\pm$ 0.04	0.385
TL	0.51 $\pm$ 0.03	0.51 $\pm$ 0.04	0.768
<b>CERAD-K</b>			
VF	17.0 $\pm$ 4.2	15.5 $\pm$ 3.1	0.070
BNT	13.2 $\pm$ 1.4	12.2 $\pm$ 1.7	0.001
MMSE	28.3 $\pm$ 1.4	28.2 $\pm$ 1.3	0.989
WLM	20.2 $\pm$ 3.2	20.3 $\pm$ 3.0	0.911
CP	10.8 $\pm$ 0.6	10.8 $\pm$ 0.8	0.976
WLR	7.0 $\pm$ 1.5	6.9 $\pm$ 1.3	0.750
WLRc	9.5 $\pm$ 0.7	9.5 $\pm$ 0.8	0.651
CR	8.4 $\pm$ 2.6	7.3 $\pm$ 2.8	0.055
TM	36.8 $\pm$ 4.7	36.7 $\pm$ 4.2	0.922
Total	86.2 $\pm$ 9.9	82.3 $\pm$ 9.1	0.063
TMT B	118.2 $\pm$ 61.6	139.8 $\pm$ 68.6	0.115
Stroop word-color	41.7 $\pm$ 10.8	39.8 $\pm$ 8.5	0.373
<b>(B) Cognitively normal older adults with positive A<math>\beta</math> deposition</b>			
<i>APOE</i> $\epsilon$ 4 carrier status	<b>Non-carrier</b>	<b>Carrier</b>	<b><i>P</i>-value</b>
	<b>(<i>n</i> = 38)</b>	<b>(<i>n</i> = 34)</b>	
Age	74.5 $\pm$ 6.6	72.5 $\pm$ 7.8	0.249
Gender			1.000
Male	11 (28.9%)	10 (29.4%)	
Female	27 (71.1%)	24 (70.6%)	
Education years	10.8 $\pm$ 4.6	11.2 $\pm$ 5.1	0.700
Global SUVR <sub>PONS</sub>	0.75 $\pm$ 0.09	0.72 $\pm$ 0.07	0.114
<b>Regional SUVR<sub>PONS</sub></b>			
ACC	0.74 $\pm$ 0.09	0.72 $\pm$ 0.09	0.319
FL	0.67 $\pm$ 0.11	0.64 $\pm$ 0.10	0.276
PL	0.58 $\pm$ 0.11	0.53 $\pm$ 0.08	0.078
PCC/precuneus	0.77 $\pm$ 0.14	0.72 $\pm$ 0.12	0.088
TL	0.69 $\pm$ 0.10	0.65 $\pm$ 0.09	0.082
<b>CERAD-K</b>			
VF	14.0 $\pm$ 4.1	15.1 $\pm$ 4.2	0.267
BNT	11.9 $\pm$ 2.2	12.1 $\pm$ 2.0	0.616
MMSE	26.7 $\pm$ 2.8	27.3 $\pm$ 2.0	0.357
WLM	17.3 $\pm$ 3.7	17.5 $\pm$ 3.8	0.802

(Continued)

**TABLE 1 |** Continued

<i>APOE</i> $\epsilon$ 4 carrier status	<b>Non-carrier</b>	<b>Carrier</b>	<b><i>P</i>-value</b>
	<b>(<i>n</i> = 38)</b>	<b>(<i>n</i> = 34)</b>	
CP	10.3 $\pm$ 1.2	10.4 $\pm$ 1.1	0.631
WLR	5.5 $\pm$ 1.7	5.5 $\pm$ 2.0	0.871
WLRc	9.0 $\pm$ 0.9	9.2 $\pm$ 0.9	0.329
CR	5.7 $\pm$ 3.0	6.6 $\pm$ 2.5	0.165
TM	31.8 $\pm$ 5.6	32.3 $\pm$ 5.9	0.707
Total	73.5 $\pm$ 13.2	76.6 $\pm$ 12.0	0.306
TMT B	196.6 $\pm$ 87.3	177.5 $\pm$ 80.4	0.338
Stroop word-color	31.5 $\pm$ 8.0	34.6 $\pm$ 13.3	0.249

Data are presented as the mean  $\pm$  standard deviation unless indicated otherwise. SUVR<sub>PONS</sub>, standardized uptake value ratios of [<sup>18</sup>F] flutemetamol (FMM), using the pons as a reference region; ACC, anterior cingulate cortex; FL, frontal lobes; PL, parietal lobes; PCC/precuneus, Posterior cingulate cortex and precuneus; TL, lateral temporal lobes; CERAD-K, Korean version of the Consortium to Establish a Registry for Alzheimer's Disease; VF, verbal fluency; BNT, Boston Naming Test; MMSE, Korean version of the Mini Mental Status Examination; WLM, word list memory; CP, constructional praxis; WLR, word list recall; WLRc, word list recognition; CR, constructional recall; TM, total scores of memory domains, including CERAD-K WLM, WLR, WLRc; Total, total scores of CERAD-K VF, BNT, WLM, CP, WLR, WLRc, and CR domains; TMT B, trail making test B.

regions with significant group differences were used for further ROI analysis.

We performed multiple regression analysis to evaluate the impact of the ReHo-by-*APOE*  $\epsilon$ 4 carrier status interaction on neuropsychological test scores. CERAD-K subdomain, TM, and total CERAD-K scores were the dependent variables, while *APOE*  $\epsilon$ 4 carrier status and zReHo values from the brain regions with significant group differences were the independent variables. Age, sex, and years of education were included as covariates. A Bonferroni correction was performed for the 12 subdomains of the CERAD-K battery (multiplying the *P*-value by a factor of 12). A significance threshold of 0.05 was used.

Furthermore, a general linear model (GLM) based on whole-brain analysis was performed on the individual z maps of ReHo to evaluate the impact of A $\beta$  deposits-by-*APOE*  $\epsilon$ 4 carrier status interaction on the local FC in each CN sub-A $\beta$  and A $\beta$ +group. The *APOE*  $\epsilon$ 4 carrier status, regional, and global FMM SUVR<sub>PONS</sub> were the independent variables. We controlled the effects of age, sex, and years of education using GLM analysis implemented in SPM 12. The threshold was set at *P* < 0.05 [false discovery rate (FDR)] to control multiple comparisons (Genovese et al., 2002).

Additionally, we applied a multiple regression analysis to examine the impact of *APOE*  $\epsilon$ 4 carrier status-by-local FC interactions on the remote FC in each CN sub-A $\beta$  and A $\beta$ +group. The dependent variables were mean z-transformed correlation values within and between the DMN, CEN, and SN, while independent variables were *APOE*  $\epsilon$ 4 carrier status and zReHo values from the brain regions with significant differences between *APOE*  $\epsilon$ 4 carriers and non-carriers. Age, sex, and years of education were included as covariates.

Finally, we performed a multiple regression analysis to evaluate the effect of *APOE*  $\epsilon 4$  carrier status-by-remote FC interactions on the cognitive function in each CN sub- $A\beta$  and  $A\beta+$  group. The CERAD-K subdomain, TM, and total CERAD-K scores were the dependent variables, while *APOE* genotype and mean z-transformed correlation values within and between the DMN, CEN, and SN were the independent variables. Age, sex, and years of education were included as covariates. We applied a threshold of  $\alpha = 0.05$ , and 0.005 to consider significant regression weights. A Bonferroni correction was additionally performed for multiple comparisons (multiplying the *P*-value by a factor of six intra- and inter-network FC). Statistical significance was set at a Bonferroni-corrected  $P < 0.05$ .

Furthermore, to exclude the effect of cortical atrophy on local and remote FC, we conducted a whole-brain voxel-wise analysis of between-group differences (*APOE*  $\epsilon 4$  carrier vs. non-carrier) in gray matter volume with a GLM using SPM12, controlling for age, sex, years of education, and intracranial volume in each CN sub- $A\beta$  and  $A\beta+$  group (**Supplementary Material**).

## RESULTS

### Baseline Demographic and Clinical Data

**Tables 1A,B** show the baseline demographic data for the CN sub- $A\beta$  and  $A\beta+$  groups. There were no significant differences in age, sex, and the number of years of education between *APOE*  $\epsilon 4$  carriers and non-carriers in either group. Regarding the global and regional FMM  $SUVR_{PONS}$ , no significant differences were found between *APOE*  $\epsilon 4$  carriers and non-carriers in each CN sub- $A\beta$  and  $A\beta+$  group. In neuropsychological test scores, *APOE*  $\epsilon 4$  non-carriers showed significantly higher scores in the CERAD-K BNT subdomains than the *APOE*  $\epsilon 4$  carriers in the CN sub- $A\beta$  group ( $P$ -value  $< 0.001$ ). However, the remaining domains, TM, and total scores showed no significant difference between *APOE*  $\epsilon 4$  carriers and non-carriers in both CN sub- $A\beta$  and  $A\beta+$  groups.

### Association Between the Quantitative Value of $A\beta$ Accumulation and Neuropsychological Test Scores According to *APOE* $\epsilon 4$ Carrier Status

**Figure 1** displays the differential associations between the regional and global  $A\beta$  accumulation and cognitive performance scores depending on the *APOE*  $\epsilon 4$  carrier status in each CN sub- $A\beta$  and  $A\beta+$  group. In the CN sub- $A\beta$  group, there was a significant interaction between *APOE*  $\epsilon 4$  carrier status and  $A\beta$  deposits such that the executive function was higher in the *APOE*  $\epsilon 4$  carrier that showed higher global and regional FMM  $SUVR_{PONS}$  in the PCC/precuneus (uncorrected  $P < 0.05$ ), yielding a large effect size. In the CN  $A\beta+$  group, there was an interaction between the *APOE*  $\epsilon 4$  carrier status and the regional FMM  $SUVR_{PONS}$  in the frontal and parietal lobes for WLM, WLR, TM, and CERAD-K total scores (uncorrected  $P <$

0.05, WLM-frontal lobe  $SUVR_{PONS}$ , and CERAD-K total-parietal lobe  $SUVR_{PONS}$ ; Bonferroni corrected  $P < 0.05$ , WLM-parietal lobe  $SUVR_{PONS}$ , WLR-parietal lobe  $SUVR_{PONS}$ , and TM-parietal lobe  $SUVR_{PONS}$ ). Lower memory and global performances were displayed in the *APOE*  $\epsilon 4$  carriers with higher regional  $A\beta$  accumulation.

### Brain Regions Showing Differences in Local Connectivity Between *APOE* $\epsilon 4$ Carriers and Non-carriers

In the CN sub- $A\beta$  group, *APOE*  $\epsilon 4$  carriers exhibited significantly higher ReHo than *APOE*  $\epsilon 4$  non-carriers did in the right precuneus, the left middle occipital gyrus, and the bilateral cerebellum crus 2 (GRF correction at a  $P$ -value of  $< 0.05$ , voxel  $P < 0.001$ ). **Table 2A** and **Figure 2A** provide an overview of the differences in the local connectivity. However, as can be seen from **Table 2B** and **Figure 2A**, the CN  $A\beta+$  group with the *APOE*  $\epsilon 4$  carrier status showed significantly lower ReHo in the right insula than did the *APOE*  $\epsilon 4$  non-carriers. Additionally, there was a significant interaction between the *APOE*  $\epsilon 4$  carrier status and ReHo in the ROIs for the neuropsychological test scores in both the CN sub- $A\beta$  and  $A\beta+$  groups (Bonferroni corrected  $P < 0.05$ ). As expected from the visual inspection of the results shown in **Figure 2B**, higher ReHo in the right cerebellum crus 2 was associated with higher executive function in the *APOE*  $\epsilon 4$  carrier of the CN sub- $A\beta$  group, but lower ReHo in the right insula was correlated with higher memory and executive function in the *APOE*  $\epsilon 4$  carrier of the CN  $A\beta+$  group.

### *APOE* $\epsilon 4$ Carrier Status-by- $A\beta$ Deposition Interaction for Local Connectivity

After adjusting for age, sex, and years of education, the  $A\beta$  deposition-by-*APOE*  $\epsilon 4$  carrier status interaction demonstrated a significant effect on ReHo in both CN sub- $A\beta$  and  $A\beta+$  groups (FDR-adjusted  $P < 0.05$ ). In the CN sub- $A\beta$  group, correlation slopes between the temporal lobe  $A\beta$  accumulation and ReHo of the ROIs were more positive for *APOE*  $\epsilon 4$  carriers than for non-carriers (**Figure 3**). However, in the CN  $A\beta+$  group, lower ReHo of the right cerebellum crus 1 was shown in the *APOE*  $\epsilon 4$  carrier with higher regional  $A\beta$  deposition in the PCC/precuneus (**Figure 3**). These anatomical locations, their corresponding MNI coordinates, and the intensities of the peak points in each cluster are shown in **Table 3**.

### Impact of Local Connectivity on Remote Connectivity Depending on *APOE* $\epsilon 4$ Carrier Status

In terms of intra- and inter-network remote FC between the DMN, CEN, and SN, there were no significant differences between *APOE*  $\epsilon 4$  carriers and non-carriers in the CN sub- $A\beta$  and  $A\beta+$  groups (Bonferroni corrected  $P > 0.05$ , **Supplementary Figures 1, 2**). In addition, for the intra-network FC of the SN and the inter-network FC between the DMN and CEN, only the CN sub- $A\beta$  group exhibited a significant

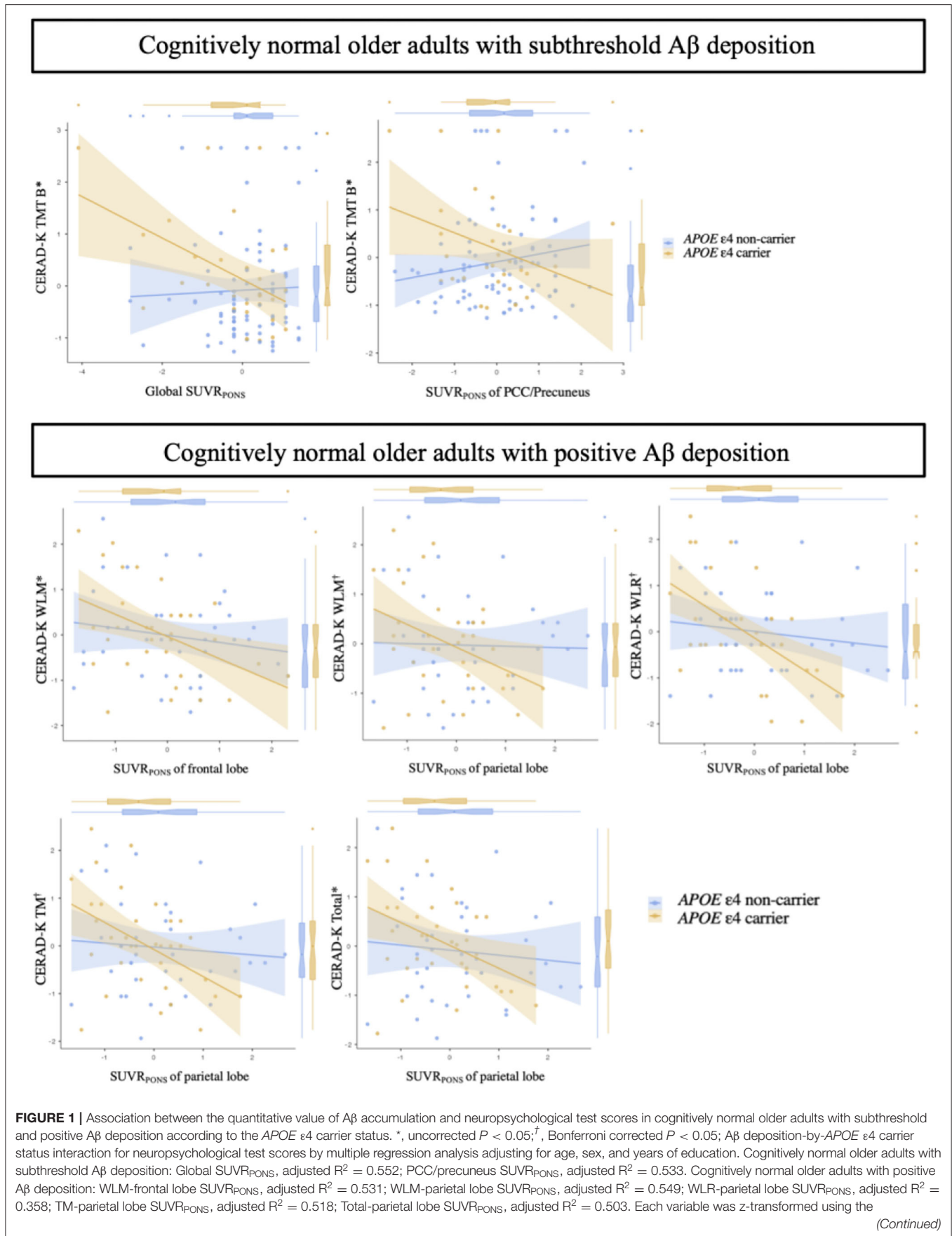


**FIGURE 1** | mean and standard deviation. CERAD-K, Korean version of the Consortium to Establish a Registry for Alzheimer's Disease; SUVR<sub>PONS</sub>, standardized uptake value ratios of [<sup>18</sup>F] flutemetamol (FMM), using the pons as a reference region; PCC/precuneus, posterior cingulate cortex and precuneus; TM, total scores of memory domains; TMT B, trail making test B; WLM, word list memory; WLR, word list recall.

**TABLE 2** | Anatomical locations of regions showing a significant difference in the regional homogeneity for cognitively normal older adults with (A) subthreshold and (B) positive A $\beta$  deposition between APOE  $\epsilon$ 4 carriers and non-carriers.

<b>(A)</b>						
Region	L/R	Cluster (Voxel count)	Peak F value	Peak MNI coordinates(x, y, z)		
<b>Significant difference in ReHo between APOE <math>\epsilon</math>4 carriers and non-carriers</b>						
Precuneus	R	66	19.1519	-10	-46	12
Cerebellum Crus 2	L	47	14.6207	-26	-82	-34
Cerebellum Crus 2	R	55	16.5878	22	-84	-36
Middle occipital gyrus	L	45	19.7821	-44	-76	14
<b>(B)</b>						
Region	L/R	Cluster (Voxel count)	Peak F value	Peak MNI coordinates (x, y, z)		
<b>Significant difference in ReHo between APOE <math>\epsilon</math>4 carriers and non-carriers</b>						
Insula	R	33	19.3333	48	2	-4

General linear model (GLM) analysis adjusted for age, sex, and years of education. Thresholds were set using GRF correction at a  $p$ -value of  $<0.05$ , voxel  $P < 0.001$ . The statistical threshold of (A) cluster size  $> 35$ , (B) cluster size  $> 29$ . L, left; R, right; ReHo, regional homogeneity.

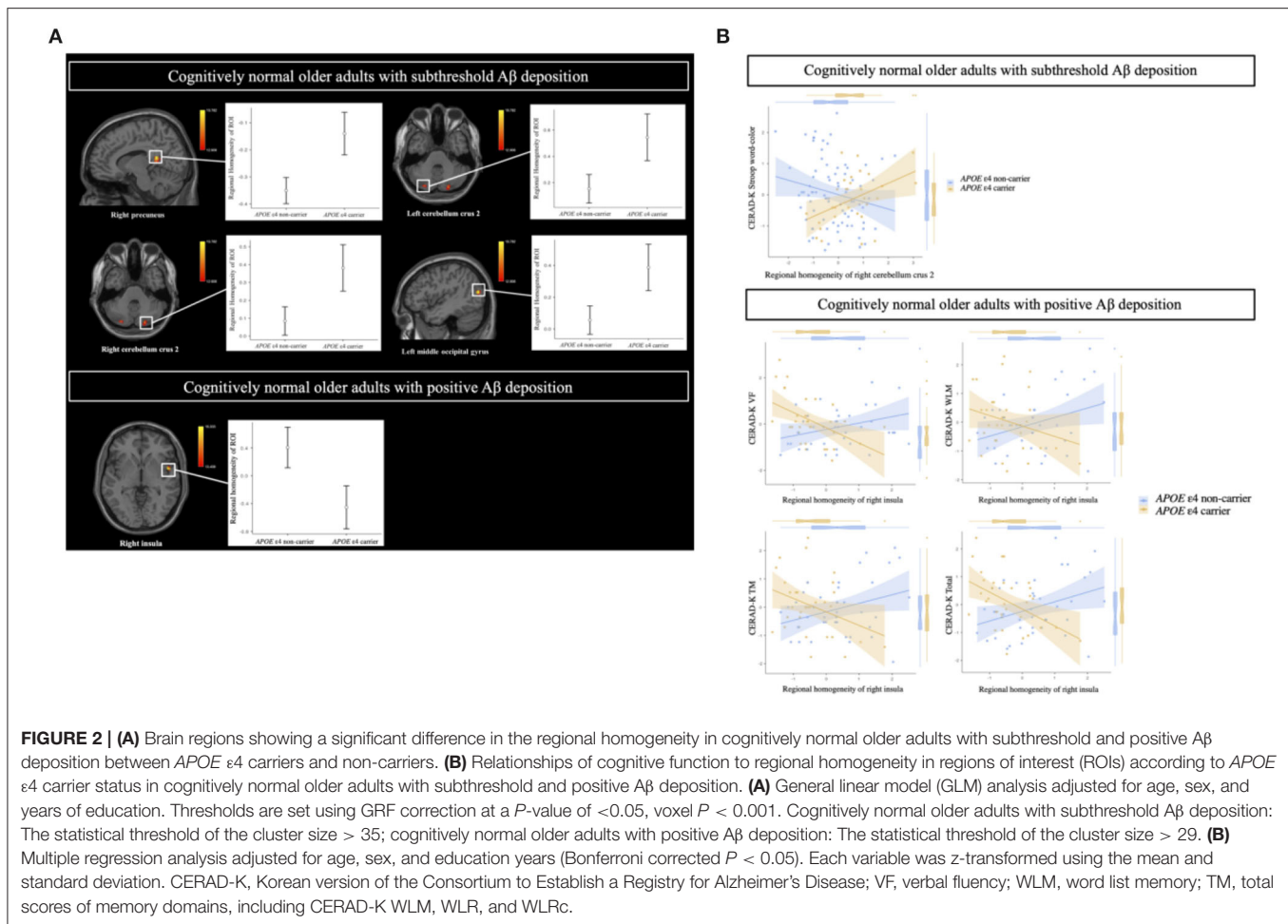
interaction between the APOE  $\epsilon$ 4 carrier status and the local connectivity in the right cerebellum crus 2, in which higher local connectivity was found in the APOE  $\epsilon$ 4 carrier than in the non-carrier group (uncorrected  $P < 0.05$ , **Figure 4A**). Although these interactions showed a large effect size, none of the interactions survived Bonferroni correction for multiple comparisons. In addition, we found a significant interaction between the APOE  $\epsilon$ 4 carrier status and the inter-network FC between the DMN and CEN for neuropsychological performance in each CN sub-A $\beta$  and A $\beta$ + group (Bonferroni corrected  $P < 0.05$ , WLM; uncorrected  $P < 0.005$ , TM; uncorrected  $P < 0.05$ , CERAD-K total and TMT B). In the CN sub-A $\beta$  group, higher memory and global performance were exhibited in the APOE  $\epsilon$ 4 carrier with a stronger inter-network FC between the DMN and CEN. In the CN A $\beta$ + group, a higher executive function was found in the APOE  $\epsilon$ 4 carrier with a stronger inter-network FC between the DMN and CEN. **Figure 4B** provides an overview of these interactions for neuropsychological performance.

## DISCUSSION

In the current study, we found a distinctive association between the regional, global A $\beta$  accumulation, and cognitive performance scores depending on the APOE  $\epsilon$ 4 carrier status in each CN sub-A $\beta$  and A $\beta$ + group. In the CN sub-A $\beta$  group, the executive

function was higher in the APOE  $\epsilon$ 4 carrier that showed higher global and regional A $\beta$  accumulation. However, lower memory and global performances were displayed in the APOE  $\epsilon$ 4 carriers with higher regional A $\beta$  deposition. Taken together, these results show that the area of cognitive function and the slope of plots between the A $\beta$  pathology and cognitive function differed according to the degree of A $\beta$  deposits in the APOE  $\epsilon$ 4 carrier in the preclinical phase. This result may also reflect the compensatory reaction in the executive function against the subthreshold A $\beta$  accumulation in the CN. Additionally, we found a significant relationship between cognitive function and A $\beta$  deposits in the posterior cortical regions. This finding broadly supports the work of a previous study demonstrating a more accurate prediction of prospective cognitive decline by A $\beta$  accumulation in the posterior brain areas than by global deposits (Farrell et al., 2018). However, this previous study could not confirm the significant impact of the APOE  $\epsilon$ 4 allele on the results. In another study, a change in the subthreshold A $\beta$  deposition was associated with memory decline but not executive function (Landau et al., 2018). In this prior study, the average age of the participants was older than that in the current study, and the presence of the APOE  $\epsilon$ 4 allele was not adjusted for the analysis. Moreover, the proportion of APOE  $\epsilon$ 4 carriers was only 15%. Therefore, such differences may have caused the discrepancy between the studies. Finally, the current study evaluated the association between A $\beta$  accumulation and





subtle cognitive decline within the normal range, which might have contributed to the relative lack of statistical robustness for the interaction.

Regarding the local FC, the *APOE*  $\epsilon 4$  carriers exhibited significantly higher ReHo, mainly in the brain region of the DMN in the CN sub-A $\beta$  group. However, there is little published research on the impact of the *APOE*  $\epsilon 4$  allele on local FC in the preclinical phase of AD. Given the positive relationship between ReHo and regional glucose metabolism (Nugent et al., 2015), *APOE*  $\epsilon 4$  carriers display increased glucose metabolism in the medial, frontal, and anterior temporal regions of the CN (Yi et al., 2014). However, this previous study did not evaluate A $\beta$  deposition, and it assessed the impact of the *APOE*  $\epsilon 4$  allele by including this high-risk genotype as the covariate in the analysis with small sample size. Another study with subjects complaining of subjective cognitive decline (SCD) showed a significant difference in the ReHo according to the A $\beta$  status. However, this previous study did not explore the interaction with the *APOE*  $\epsilon 4$  allele; it included subjects who were older than those in the present study, and also performed the analysis in the restricted sample size (Li et al., 2021). These previous results, therefore, need to be interpreted with caution regarding possible bias.

Among the ROIs showing a significantly higher ReHo in the *APOE*  $\epsilon 4$  carrier of the CN sub-A $\beta$  group, the precuneus is the known hub region of the DMN, and the ReHo in this region reflects the progression of AD (He et al., 2007; Kang et al., 2017). Although prior research has documented the negative relationship between A $\beta$  deposition and ReHo of the precuneus in the CN with a positive A $\beta$  PET scan, another previous study has demonstrated that SCD subjects with A $\beta$  deposits show a higher ReHo in the right precuneus than those without A $\beta$  accumulation, suggesting the compensatory role of the increased local FC (Li et al., 2021). However, given the A $\beta$ -dependent neuronal hyperactivation (Zott et al., 2019), we could not rule out the possibility that early A $\beta$  deposition induced a higher ReHo in the AD vulnerable brain region.

However, despite the importance of the *APOE*  $\epsilon 4$  allele, there remains a paucity of evidence on the effect of the *APOE*  $\epsilon 4$  allele on the local FC change in the earliest phase of AD. Concerning the middle occipital gyrus, which is another ROI in the CN sub-A $\beta$  group, the FC between this ROI and precuneus has been shown to be higher in SCD subjects with A $\beta$  burden than in those without A $\beta$  deposits (Li et al., 2021). Additionally, we found a higher ReHo in several posterior regions of the cerebellum in the *APOE*  $\epsilon 4$  carriers in the CN sub-A $\beta$  group. The posterior

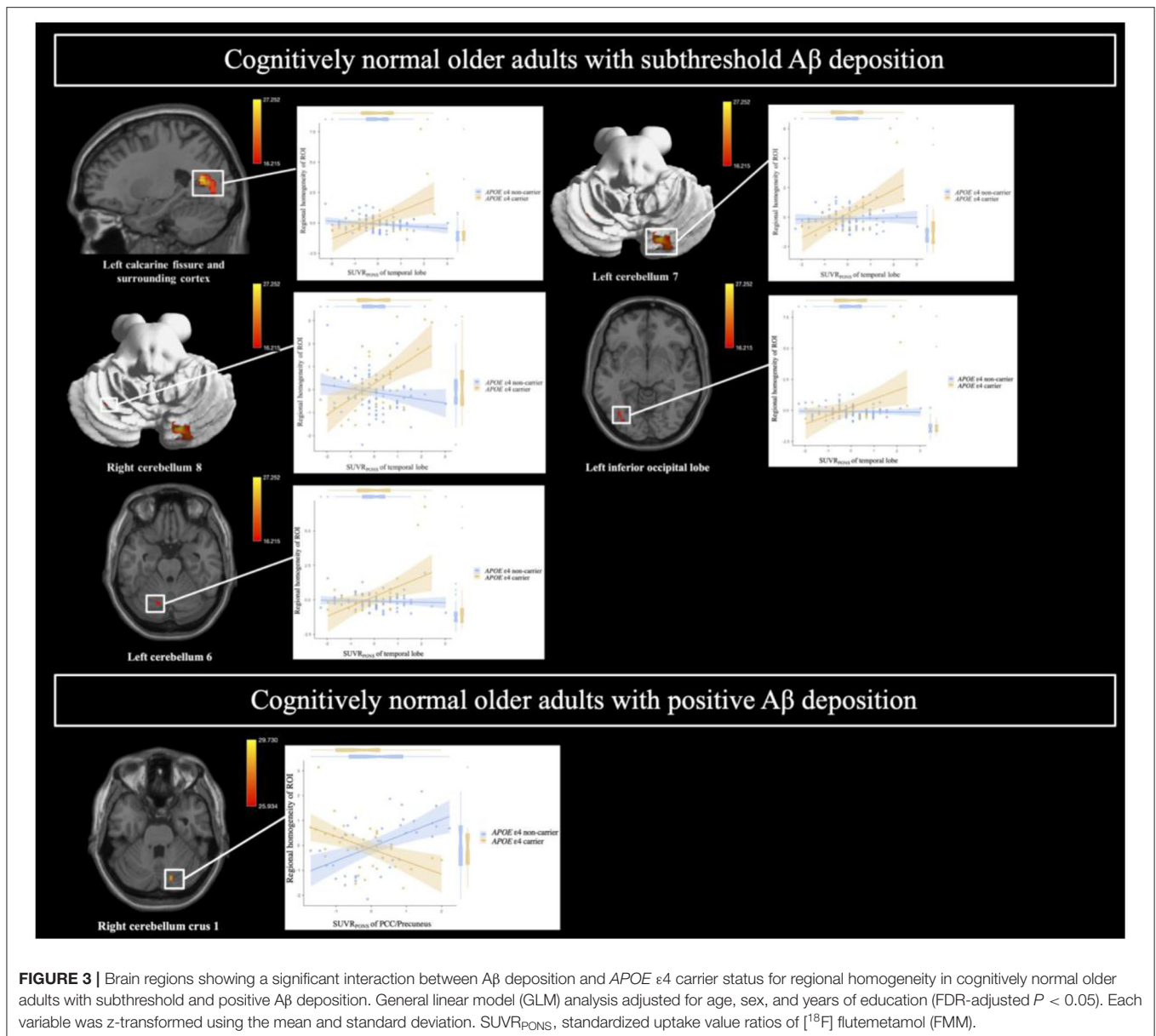


**FIGURE 3** | Brain regions showing a significant interaction between A $\beta$  deposition and APOE  $\epsilon$ 4 carrier status for regional homogeneity in cognitively normal older adults with subthreshold and positive A $\beta$  deposition. General linear model (GLM) analysis adjusted for age, sex, and years of education (FDR-adjusted  $P < 0.05$ ). Each variable was z-transformed using the mean and standard deviation. SUVR<sub>PONS</sub>, standardized uptake value ratios of [<sup>18</sup>F] flutemetamol (FMM).

cerebellum has been reported to be functionally mapped to the DMN brain regions (Buckner et al., 2011; Buckner, 2013) that are prone to A $\beta$  accumulation (Mormino et al., 2011). In this regard, the A $\beta$ -associated neuronal hyperactivation might affect the high activity of the DMN brain regions and functionally related posterior cerebellum (Pasquini et al., 2017). Additionally, neuronal hyperactivity has also been reported to induce further A $\beta$  deposition (Bero et al., 2012). This positive correspondence between A $\beta$  and intrinsic FC has been demonstrated to start in the preclinical stage (Pasquini et al., 2017). Additionally, a previous study has also shown the impact of the APOE  $\epsilon$ 4 allele on neuronal hyperactivity in a mouse model without definite A $\beta$  pathology (Nuriel et al., 2017). Therefore, a synergistic effect of the APOE  $\epsilon$ 4 allele with the A $\beta$  burden could affect the high activity of the ROIs in the current study. However,

the posterior cerebellum did not show a significant difference depending on the APOE  $\epsilon$ 4 carrier status in the CN A $\beta$ + group of the present study. The detrimental effect of A $\beta$  on FC has been reported to appear in brain networks where both the brain activity and A $\beta$  deposits are high (Pasquini et al., 2017). In addition, this deteriorating effect has been reported to initiate already in the preclinical phase and reach a peak in the MCI stage (Pasquini et al., 2017). In this regard, a higher A $\beta$  burden might weaken the brain activity of the ROIs in the CN A $\beta$ + group. However, a further longitudinal study is required to determine exactly how A $\beta$  influences the brain functional change, conjoining with APOE  $\epsilon$ 4 allele in the preclinical phase.

In the CN A $\beta$ + group in the present study, the APOE  $\epsilon$ 4 carriers showed significantly lower ReHo in the insula, which is a

**TABLE 3** | Anatomical locations of regions showing a significant interaction between A $\beta$  deposition and APOE  $\epsilon$ 4 carrier status for regional homogeneity in cognitively normal older adults with (A) subthreshold and (B) positive A $\beta$  deposition.

<b>(A)</b>						
Region	L/R	Cluster (Voxel count)	Peak F-value	Peak MNI coordinates (x, y, z)		
<b>Temporal lobe SUVR<sub>PONS</sub>-by-APOE <math>\epsilon</math>4 carrier status interaction for regional homogeneity</b>						
Calcarine fissure and surrounding cortex	L	323	27.2528	-26	-64	12
Cerebellum 7	L	148	26.3141	-14	-76	-46
Cerebellum 8	R	50	23.5239	24	-64	-54
Inferior occipital lobe	L	49	19.5212	-36	-70	-4
Cerebellum 6	L	34	17.874	-18	-66	-24
<b>(B)</b>						
Region	L/R	Cluster (Voxel count)	Peak F value	Peak MNI coordinates (x, y, z)		
<b>PCC/precuneus SUVR<sub>PONS</sub>-by-APOE <math>\epsilon</math>4 carrier status interaction for regional homogeneity</b>						
Cerebellum Crus 1	R	23	29.7307	16	-78	-24

General linear model (GLM) analysis adjusted for age, sex, years of education, FDR-adjusted  $P < 0.05$ , SUVR<sub>PONS</sub>, standardized uptake value ratios of [<sup>18</sup>F] flutemetamol (FMM); L, left; R, right; PCC/precuneus, posterior cingulate cortex and precuneus; SUVR<sub>PONS</sub>, standardized uptake value ratios of [<sup>18</sup>F] FMM, using the pons as a reference region.

known hub region of the SN. The insula has been demonstrated to have a modulatory role in the association between the DMN and CEN (Sridharan et al., 2008). Additionally, the SN has been documented to display distinctive FC activation from normal aging to AD progression (He et al., 2014). Contrary to the current findings, the APOE  $\epsilon$ 4 carrier in the preclinical phase has demonstrated increased FC related to the insula, which is attributed to the reduction of the inhibitory control of the DMN (Machulda et al., 2011). However, in the present study, there were no significant differences in the intra-network FC of the DMN and the inter-network FC between the DMN and SN depending on the APOE  $\epsilon$ 4 carrier status in the CN A $\beta$ + group. Nevertheless, caution should be exercised here because there was a lack of information on A $\beta$  deposition in the above-mentioned previous studies, and the difference in the ReHo has been shown depending on A $\beta$  positivity during the preclinical phase (Kang et al., 2017).

In the present study, the difference in ReHo in the APOE  $\epsilon$ 4 carriers was related to the higher executive and memory function in each CN sub-A $\beta$  and CN A $\beta$ + group, respectively. Additionally, this finding broadly supports the work of other studies linking the functional activation of the posterior cerebellum with executive function (Baumann et al., 2015; Castellazzi et al., 2018). In this regard, this combination of findings provides some support for the compensatory role of the difference in the ReHo found in the APOE  $\epsilon$ 4 carriers in the preclinical phase. However, these results differ from some published studies reporting a non-significant association between FC and cognitive function in APOE  $\epsilon$ 4 carriers with intact cognition

(Chen et al., 2015). These differences can be explained in part by not considering the effect of the A $\beta$  burden in the previous study.

Another interesting finding was the differential association between regional A $\beta$  burden and local connectivity according to the APOE  $\epsilon$ 4 carrier status in each CN sub-A $\beta$  and A $\beta$ + group. In the APOE  $\epsilon$ 4 carriers in the CN sub-A $\beta$  group, the ReHo was higher in ROI, including the posterior cerebellum, as the A $\beta$  accumulation in the temporal lobe was higher, but in the CN A $\beta$ + group, the ReHo was lower in the right cerebellum crus 1 as the A $\beta$  burden in the PCC/precuneus was higher. Although the subjects of this study were not in the age group in which A $\beta$  deposition was actively increasing (Rodrigue et al., 2012), the temporal lobe and PCC/precuneus have been reported as early A $\beta$  deposition regions (Sojkova et al., 2011). These regions have been demonstrated to be vulnerable to the APOE  $\epsilon$ 4 allele (Sheline et al., 2010) and to show an overlap between the topological distribution of A $\beta$  deposits and the DMN (Kang et al., 2017). Additionally, hyperactivity in these regions has been assumed to induce further A $\beta$  accumulation, which could cause neuronal dysfunction and reduced FC in the CN (Bero et al., 2011, 2012). In addition, among the ROIs in the current findings, the posterior cerebellum has been demonstrated to be functionally connected to the temporal gyrus and precuneus, which are the vulnerable regions in AD (Guo et al., 2016). Significantly, the cerebellum crus 1 and cerebellum 7 have also been mapped to the DMN brain regions (Buckner et al., 2011), including the association cortex where A $\beta$  accumulation is prone to occur (Mormino et al., 2011). However, few previous studies on the distinctive effect of the

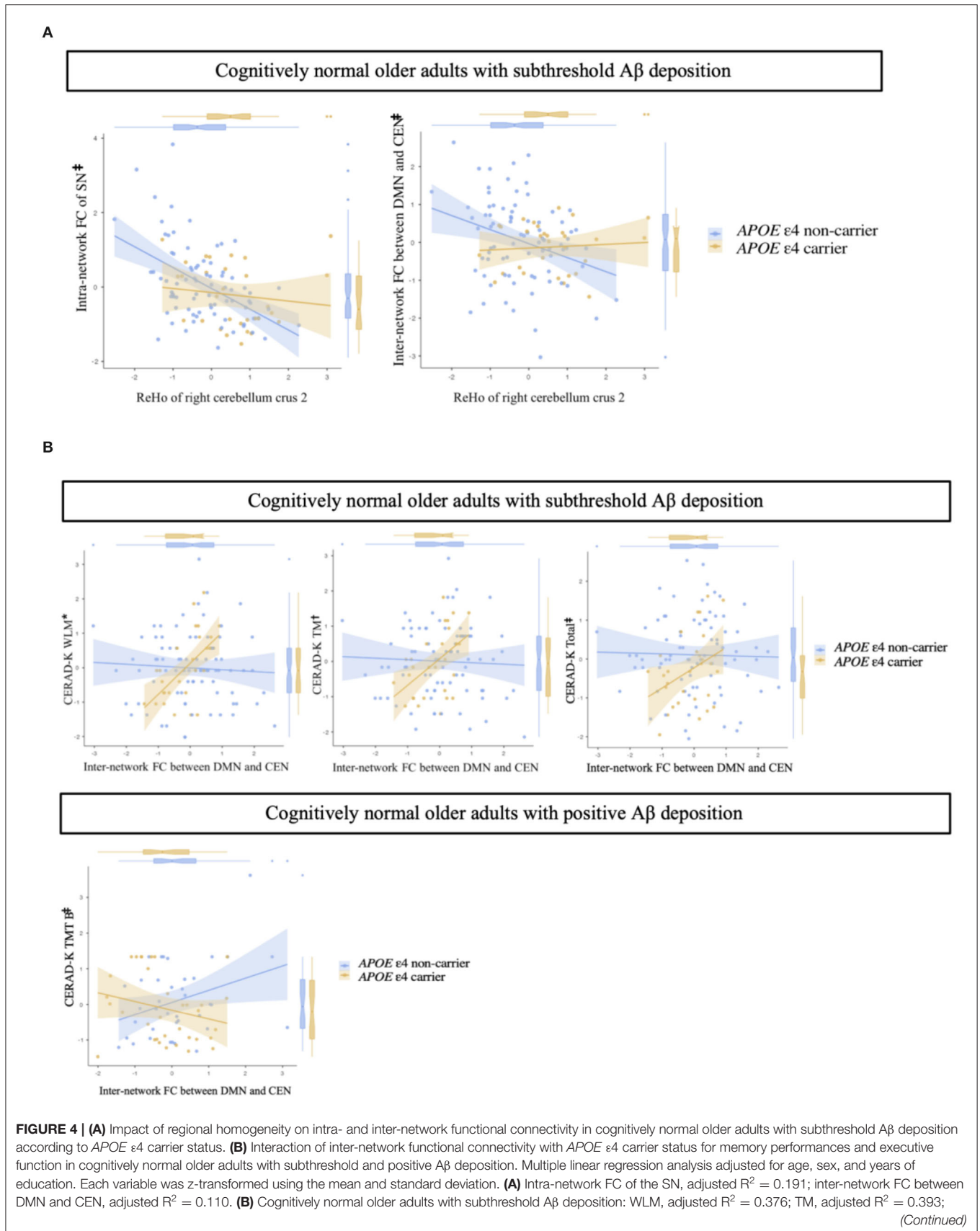


**FIGURE 4** | Total, adjusted  $R^2 = 0.521$ . Cognitively normal older adults with positive A $\beta$  deposition: TMT B, adjusted  $R^2 = 0.365$ . \*, Bonferroni corrected  $P < 0.05$ ; †, uncorrected  $P < 0.005$ ; ‡, uncorrected  $P < 0.05$ . FC, functional connectivity; SN, salience network; DMN, default-mode network; CEN, central-executive network; CERAD-K, the Korean version of the Consortium to Establish a Registry for Alzheimer's Disease; WLM, word list memory; TM, total scores of memory domains; total, total scores summing up all subcategory scores, excluding the MMSE score; TMT B, trail making test B.

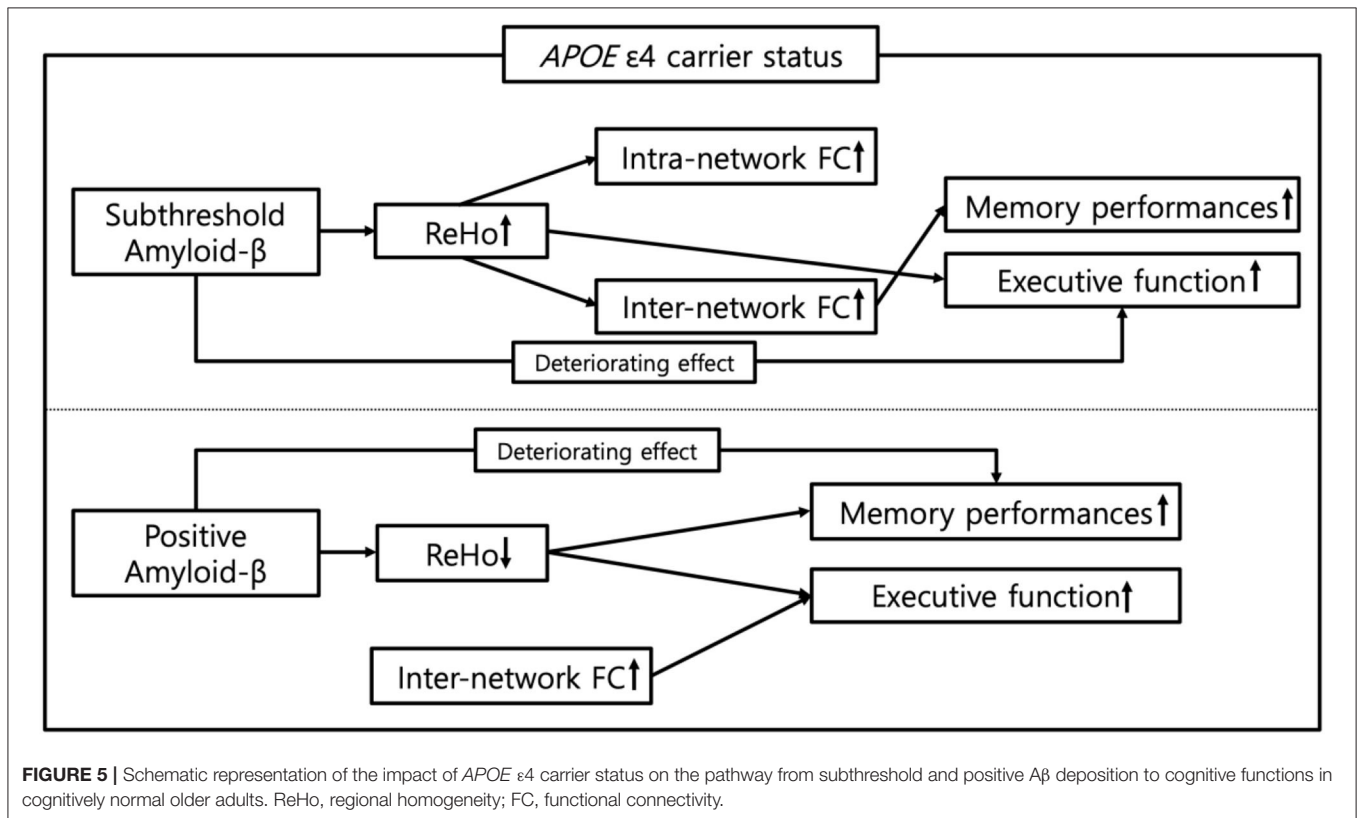


**FIGURE 5** | Schematic representation of the impact of *APOE*  $\epsilon 4$  carrier status on the pathway from subthreshold and positive A $\beta$  deposition to cognitive functions in cognitively normal older adults. ReHo, regional homogeneity; FC, functional connectivity.

*APOE*  $\epsilon 4$  allele on the function of the posterior cerebellum have been performed. Therefore, starting from this study, additional reproducible studies are needed to verify the differential effects of the *APOE*  $\epsilon 4$  allele. Furthermore, the temporal gyrus has also been known to be correlated with tau pathology (Insel et al., 2020) and a synergistic effect between A $\beta$  and tauopathy for the changes in the FC has been reported (Schultz et al., 2017). Therefore, additional studies evaluating tauopathy are necessary to understand the earliest pathophysiology of AD more accurately.

In the CN sub-A $\beta$  group of the present study, there was a significant interaction between the *APOE*  $\epsilon 4$  carrier status and local FC in the right cerebellum crus 2 for the remote inter-network FC between the DMN and CEN, showing robustness to the decline in this inter-network FC in the *APOE*  $\epsilon 4$  carriers. This is consistent with previous findings showing a significant association between the posterior cerebellum and resting-state networks, including the DMN and CEN (Habas et al., 2009; Buckner et al., 2011). The inter-network FC between the DMN and CEN has been reported to display a U-shaped progression pattern with increasing age, and to show a declining pattern in the age group of the subjects in the current study (Ng et al., 2016).

In this regard, the *APOE*  $\epsilon 4$  carrier status could be suggested to have an alleviating role for this declining pattern in the CN before the A $\beta$  positivity. Furthermore, we found that the stronger inter-network FC of DMN-CEN was associated with better cognitive function in the *APOE*  $\epsilon 4$  carrier in both CN sub-A $\beta$  and A $\beta$ + groups. The function of the CEN has been demonstrated to be supported by that of the DMN in maintaining a normal cognition (Turner and Spreng, 2015). In this respect, the present results support previous observational studies that have shown a positive association between the cognitive function and the inter-network FC of DMN-CEN in the cognitively normal *APOE*  $\epsilon 4$  carrier of similar age to the present study (Ng et al., 2018).

In the current study, the participants with varying risk for AD have not yet been confirmed to have developed further A $\beta$  accumulation or converted to symptomatic disease. Moreover, considering the results of previous studies showing that A $\beta$  changes rather than that baseline accumulation predicts prospective cognitive change (Farrell et al., 2018); accordingly, it is necessary to conduct a longitudinal study for a clear interpretation of the results of the current study. Given that prior study has demonstrated an interaction between A $\beta$  and

tau for changes in the FC of the CN (Hasani et al., 2021), another issue with this study is the lack of information on the tau deposits. Additionally, it has been reported that the FMM has a relatively low sensitivity to diffuse plaques that are usually detected in the earliest phase of A $\beta$  accumulation (Salloway et al., 2017). In this respect, the current findings must be interpreted with caution when comparing them with the results of previous studies using other types of A $\beta$  ligands. In addition, a selection bias is another potential limitation. The APOE  $\epsilon$ 4 carriers whose cognitive function remained intact despite the A $\beta$  burden could have other characteristics, including protective genes (Seto et al., 2021) and higher cognitive reserve (Stern, 2009). The characteristics of these participants might have influenced the non-significant difference in cognitive function according to APOE  $\epsilon$ 4 carrier status. Finally, in the present study, multiple analyzes were performed after dichotomization according to A $\beta$  positivity due to many analysis variables. Additionally, conventional data-fusion methods have difficulty in capturing complex relationships between multiple data, including brain imaging, genetic, demographic, and clinical data (Hu et al., 2019). In this regard, we need to apply deep collaborative learning, which can link the whole data simultaneously to develop a complete understanding of the A $\beta$  pathophysiological cascade during the preclinical phase (Song and Chai, 2018; Hu et al., 2019). This novel method has been demonstrated to improve the generalization and robustness of brain research (Song and Chai, 2018).

## CONCLUSION

The present study was designed to explore the distinctive effect of the APOE  $\epsilon$ 4 carrier status on the associations between subthreshold, positive A $\beta$  deposition, FC, and cognitive performance during the preclinical phase. We have depicted the impact of the APOE  $\epsilon$ 4 carrier status on the pathway from the subthreshold and positive A $\beta$  deposits to cognitive performance *via* the local and remote FC, as illustrated in the schematic in **Figure 5**. Finally, this new understanding based on the APOE  $\epsilon$ 4 carrier status should help to improve predictions of the impact of the earliest A $\beta$  accumulation on the progression of AD with a compliment to the aforementioned limitations.

## REFERENCES

- Abrol, A., Damaraju, E., Miller, R. L., Stephen, J. M., Claus, E. D., Mayer, A. R., et al. (2017). Replicability of time-varying connectivity patterns in large resting state fMRI samples. *Neuroimage* 163, 160–176. doi: 10.1016/j.neuroimage.2017.09.020
- Andrews-Zwilling, Y., Bien-Ly, N., Xu, Q., Li, G., Bernardo, A., Yoon, S. Y., et al. (2010). Apolipoprotein E4 causes age- and Tau-dependent impairment of GABAergic interneurons, leading to learning and memory deficits in mice. *J. Neurosci.* 30, 13707–13717. doi: 10.1523/JNEUROSCI.4040-10.2010
- Baker, J. E., Lim, Y. Y., Pietrzak, R. H., Hassenstab, J., Snyder, P. J., Masters, C. L., et al. (2017). Cognitive impairment and decline in cognitively normal older adults with high amyloid- $\beta$ : a meta-analysis. *Alzheimers*

## DATA AVAILABILITY STATEMENT

The datasets generated or analyzed during the current study are not publicly available because of the Patient Data Management Protocol of Yeouido Saint Mary's Hospital, but are available from the corresponding author upon reasonable request.

## ETHICS STATEMENT

The studies involving human participants were reviewed and approved by Institutional Review Board of the Catholic University of Korea. The patients/participants provided their written informed consent to participate in this study.

## AUTHOR CONTRIBUTIONS

DK contributed to conceptualization, methodology, data curation, writing the original draft, visualization, formal analysis, and funding acquisition. S-MW contributed to methodology, data curation, and writing, reviewing, and editing the manuscript. YU contributed to software and investigation. N-YK contributed to methodology and data curation. CL contributed to conceptualization and supervision. HL contributed to conceptualization, methodology, supervision, project administration, funding acquisition, and writing, reviewing, and editing the manuscript. All authors contributed to the article and approved the submitted version.

## FUNDING

This work was supported by the National Research Foundation of Korea grants funded by the Korean government (Ministry of Science and ICT) (Nos. 2019R1A2C2009100 and 2019R1C1C1007608). The funders had no role in the study design, data collection and analysis, decision to publish, or preparation of the manuscript.

## SUPPLEMENTARY MATERIAL

The Supplementary Material for this article can be found online at: <https://www.frontiersin.org/articles/10.3389/fnagi.2022.871323/full#supplementary-material>

*Dement. Diag. Assess. Dis. Monit.* 6, 108–121. doi: 10.1016/j.dadm.2016.09.002

- Bansal, R., and Peterson, B. S. (2018). Cluster-level statistical inference in fMRI datasets: the unexpected behavior of random fields in high dimensions. *Magn. Reson. Imaging* 49, 101–115. doi: 10.1016/j.mri.2018.01.004
- Baumann, O., Borra, R. J., Bower, J. M., Cullen, K. E., Habas, C., Ivry, R. B., et al. (2015). Consensus paper: the role of the cerebellum in perceptual processes. *Cerebellum* 14, 197–220. doi: 10.1007/s12311-014-0627-7
- Bero, A. W., Bauer, A. Q., Stewart, F. R., White, B. R., Cirrito, J. R., Raichle, M. E., et al. (2012). Bidirectional relationship between functional connectivity and amyloid- $\beta$  deposition in mouse brain. *J. Neurosci.* 32, 4334–4340. doi: 10.1523/JNEUROSCI.5845-11.2012

- Bero, A. W., Yan, P., Roh, J. H., Cirrito, J. R., Stewart, F. R., Raichle, M. E., et al. (2011). Neuronal activity regulates the regional vulnerability to amyloid- $\beta$  deposition. *Nat. Neurosci.* 14, 750–756. doi: 10.1038/nn.2801
- Bien-Ly, N., Andrews-Zwilling, Y., Xu, Q., Bernardo, A., Wang, C., and Huang, Y. (2011). C-terminal-truncated apolipoprotein (apo) E4 inefficiently clears amyloid- $\beta$  (A $\beta$ ) and acts in concert with A $\beta$  to elicit neuronal and behavioral deficits in mice. *Proc. Nat. Acad. Sci.* 108, 4236–4241. doi: 10.1073/pnas.1018381108
- Bischof, G. N., and Jacobs, H. I. (2019). Subthreshold amyloid and its biological and clinical meaning: long way ahead. *Neurology* 93, 72–79. doi: 10.1212/WNL.00000000000007747
- Biswal, B. B., Mennes, M., Zuo, X. N., Gohel, S., Kelly, C., Smith, S. M., et al. (2010). Toward discovery science of human brain function. *Proc. Natl. Acad. Sci. U. S. A.* 107, 4734–4739. doi: 10.1073/pnas.0911855107
- Brier, M. R., Thomas, J. B., Snyder, A. Z., Benzinger, T. L., Zhang, D., Raichle, M. E., et al. (2012). Loss of intranetwork and internetwork resting state functional connections with Alzheimer's disease progression. *J. Neurosci.* 32, 8890–8899. doi: 10.1523/JNEUROSCI.5698-11.2012
- Buckner, R. L. (2004). Memory and executive function in aging and AD: multiple factors that cause decline and reserve factors that compensate. *Neuron* 44, 195–208. doi: 10.1016/j.neuron.2004.09.006
- Buckner, R. L. (2013). The cerebellum and cognitive function: 25 years of insight from anatomy and neuroimaging. *Neuron* 80, 807–815. doi: 10.1016/j.neuron.2013.10.044
- Buckner, R. L., Krienen, F. M., Castellanos, A., Diaz, J. C., and Yeo, B. T. (2011). The organization of the human cerebellum estimated by intrinsic functional connectivity. *J. Neurophysiol.* 106, 2322–2345. doi: 10.1152/jn.00339.2011
- Castellano, J. M., Kim, J., Stewart, F. R., Jiang, H., Demattos, R. B., Patterson, B. W., et al. (2011). Human apoE isoforms differentially regulate brain amyloid- $\beta$  peptide clearance. *Sci. Transl. Med.* 3, 89ra57. doi: 10.1126/scitranslmed.3002156
- Castellazzi, G., Bruno, S. D., Toosy, A. T., Casiraghi, L., Palesi, F., Savini, G., et al. (2018). Prominent changes in cerebello-cerebellar functional connectivity during continuous cognitive processing. *Front. Cell. Neurosci.* 12, 331. doi: 10.3389/fncel.2018.00331
- Chen, Y., Chen, K., Zhang, J., Li, X., Shu, N., Wang, J., et al. (2015). Disrupted functional and structural networks in cognitively normal elderly subjects with the APOE  $\epsilon$  4 allele. *Neuropsychopharmacology* 40, 1181–1191. doi: 10.1038/npp.2014.302
- Corder, E. H., Saunders, A. M., Strittmatter, W. J., Schmechel, D. E., Gaskell, P. C., Small, G. W., et al. (1993). Gene dose of apolipoprotein E type 4 allele and the risk of Alzheimer's disease in late onset families. *Science* 261, 921–923. doi: 10.1126/science.8346443
- Deco, G., Ponce-Alvarez, A., Hagmann, P., Romani, G. L., Mantini, D., and Corbetta, M. (2014). How local excitation-inhibition ratio impacts the whole brain dynamics. *J. Neurosci.* 34, 7886–7898. doi: 10.1523/JNEUROSCI.5068-13.2014
- DeMattos, R. B., Cirrito, J. R., Parsadanian, M., May, P. C., O'dell, M. A., Taylor, J. W., et al. (2004). ApoE and clusterin cooperatively suppress Abeta levels and deposition: evidence that ApoE regulates extracellular Abeta metabolism *in vivo*. *Neuron* 41, 193–202. doi: 10.1016/S0896-6273(03)00850-X
- Driscoll, I., Troncoso, J. C., Rudow, G., Sojkova, J., Pletnikova, O., Zhou, Y., et al. (2012). Correspondence between *in vivo* 11C-PiB-PET amyloid imaging and postmortem, region-matched assessment of plaques. *Acta Neuropathol.* 124, 823–831. doi: 10.1007/s00401-012-1025-1
- Farrell, M. E., Chen, X., Rundle, M. M., Chan, M. Y., Wig, G. S., and Park, D. C. (2018). Regional amyloid accumulation and cognitive decline in initially amyloid-negative adults. *Neurology* 91, e1809–e1821. doi: 10.1212/WNL.00000000000006469
- Farrell, M. E., Jiang, S., Schultz, A. P., Properzi, M. J., Price, J. C., Becker, J. A., et al. (2021). Defining the lowest threshold for amyloid-PET to predict future cognitive decline and amyloid accumulation. *Neurology* 96, e619–e631. doi: 10.1212/WNL.00000000000011214
- Frisoni, G. B., Altomare, D., Thal, D. R., Ribaldi, F., Van Der Kant, R., Ossenkoppele, R., et al. (2022). The probabilistic model of Alzheimer disease: the amyloid hypothesis revised. *Nat. Rev. Neurosci.* 23, 53–66. doi: 10.1038/s41583-021-00533-w
- Genovese, C. R., Lazar, N. A., and Nichols, T. (2002). Thresholding of statistical maps in functional neuroimaging using the false discovery rate. *Neuroimage* 15, 870–878. doi: 10.1006/nimg.2001.1037
- Guo, C. C., Tan, R., Hodges, J. R., Hu, X., Sami, S., and Hornberger, M. (2016). Network-selective vulnerability of the human cerebellum to Alzheimer's disease and frontotemporal dementia. *Brain* 139, 1527–1538. doi: 10.1093/brain/aww003
- Habas, C., Kamdar, N., Nguyen, D., Prater, K., Beckmann, C. F., Menon, V., et al. (2009). Distinct cerebellar contributions to intrinsic connectivity networks. *J. Neurosci.* 29, 8586–8594. doi: 10.1523/JNEUROSCI.1868-09.2009
- Hahn, A., Strandberg, T. O., Stomrud, E., Nilsson, M., Van Westen, D., Palmqvist, S., et al. (2019). Association between earliest amyloid uptake and functional connectivity in cognitively unimpaired elderly. *Cerebral Cortex* 29, 2173–2182. doi: 10.1093/cercor/bhz020
- Hasani, S. A., Mayeli, M., Salehi, M. A., and Barzegar Parizi, R. (2021). A systematic review of the association between amyloid- $\beta$  and  $\tau$  pathology with functional connectivity alterations in the Alzheimer dementia spectrum utilizing PET scan and rsfMRI. *Dement. Geriatr. Cogn. Dis. Extra* 11, 78–90. doi: 10.1159/000516164
- He, X., Qin, W., Liu, Y., Zhang, X., Duan, Y., Song, J., et al. (2014). Abnormal salience network in normal aging and in amnesic mild cognitive impairment and Alzheimer's disease. *Hum. Brain Mapp.* 35, 3446–3464. doi: 10.1002/hbm.22414
- He, Y., Wang, L., Zang, Y., Tian, L., Zhang, X., Li, K., et al. (2007). Regional coherence changes in the early stages of Alzheimer's disease: a combined structural and resting-state functional MRI study. *Neuroimage* 35, 488–500. doi: 10.1016/j.neuroimage.2006.11.042
- Hedden, T., Van Dijk, K. R., Becker, J. A., Mehta, A., Sperling, R. A., Johnson, K. A., et al. (2009). Disruption of functional connectivity in clinically normal older adults harboring amyloid burden. *J. Neurosci.* 29, 12686–12694. doi: 10.1523/JNEUROSCI.3189-09.2009
- Hu, W., Cai, B., Zhang, A., Calhoun, V. D., and Wang, Y.-P. (2019). Deep collaborative learning with application to the study of multimodal brain development. *IEEE Trans. Biomed. Eng.* 66, 3346–3359. doi: 10.1109/TBME.2019.2904301
- Hutchinson, R. M., Womelsdorf, T., Allen, E. A., Bandettini, P. A., Calhoun, V. D., Corbetta, M., et al. (2013). Dynamic functional connectivity: promise, issues, and interpretations. *Neuroimage* 80, 360–378. doi: 10.1016/j.neuroimage.2013.05.079
- Insel, P. S., Mormino, E. C., Aisen, P. S., Thompson, W. K., and Donohue, M. C. (2020). Neuroanatomical spread of amyloid  $\beta$  and tau in Alzheimer's disease: implications for primary prevention. *Brain Commun.* 2, fcaa007. doi: 10.1093/braincomms/fcaa007
- Insel, P. S., Ossenkoppele, R., Gessert, D., Jagust, W., Landau, S., Hansson, O., et al. (2017). Time to amyloid positivity and preclinical changes in brain metabolism, atrophy, and cognition: evidence for emerging amyloid pathology in Alzheimer's disease. *Front. Neurosci.* 11, 281. doi: 10.3389/fnins.2017.00281
- Jack, C. R., Bennett, D. A., Blennow, K., Carrillo, M. C., Dunn, B., Haeberlein, S. B., et al. (2018). NIA-AA research framework: toward a biological definition of Alzheimer's disease. *Alzheimers Dement.* 14, 535–562. doi: 10.1016/j.jalz.2018.02.018
- Jack, C. R., Knopman, D. S., Jagust, W. J., Petersen, R. C., Weiner, M. W., Aisen, P. S., et al. (2013). Tracking pathophysiological processes in Alzheimer's disease: an updated hypothetical model of dynamic biomarkers. *Lancet Neurol.* 12, 207–216. doi: 10.1016/S1474-4422(12)70291-0
- Jiang, L., and Zuo, X. N. (2016). Regional homogeneity: a multimodal, multiscale neuroimaging marker of the human connectome. *Neuroscientist* 22, 486–505. doi: 10.1177/1073858415595004
- Kang, D. W., Choi, W. H., Jung, W. S., Um, Y. H., Lee, C. U., and Lim, H. K. (2017). Impact of amyloid burden on regional functional synchronization in the cognitively normal older adults. *Sci. Rep.* 7, 14690. doi: 10.1038/s41598-017-15001-8
- Kang, D. W., Wang, S. M., Um, Y. H., Na, H. R., Kim, N. Y., Lee, C. U., et al. (2021). Distinctive association of the functional connectivity of the posterior cingulate cortex on memory performances in early and late amnesic mild cognitive impairment patients.

- Front. Aging Neurosci. 13, 696735. doi: 10.3389/fnagi.2021.696735
- Kendall, M., and Gibbons, J. (1990). *Rank Correlation Methods*. London: Oxford University Press.
- Knopman, D. S., Jack, C. R. Jr., Wiste, H. J., Weigand, S. D., Vemuri, P., Lowe, V., et al. (2012). Short-term clinical outcomes for stages of NIA-AA preclinical Alzheimer disease. *Neurology* 78, 1576–1582. doi: 10.1212/WNL.0b013e3182563bbe
- Landau, S. M., Horng, A., and Jagust, W. J. (2018). Memory decline accompanies subthreshold amyloid accumulation. *Neurology* 90, e1452–e1460. doi: 10.1212/WNL.0000000000005354
- Laumann, T. O., Snyder, A. Z., Mitra, A., Gordon, E. M., Gratton, C., Adeyemo, B., et al. (2017). On the stability of BOLD fMRI correlations. *Cerebral Cortex* 27, 4719–4732. doi: 10.1093/cercor/bhw265
- Leal, S. L., Lockhart, S. N., Maass, A., Bell, R. K., and Jagust, W. J. (2018). Subthreshold amyloid predicts tau deposition in aging. *J. Neurosci.* 38, 4482–4489. doi: 10.1523/JNEUROSCI.0485-18.2018
- Lee, J. H., Lee, K. U., Lee, D. Y., Kim, K. W., Jhoo, J. H., Kim, J. H., et al. (2002). Development of the Korean version of the consortium to Establish a Registry for Alzheimer's disease assessment packet (CERAD-K): clinical and neuropsychological assessment batteries. *J. Gerontol. B Psychol. Sci. Soc. Sci.* 57, P47–53. doi: 10.1093/geronb/57.1.P47
- Li, S., Daamen, M., Scheef, L., Gaertner, F. C., Buchert, R., Buchmann, M., et al. (2021). Abnormal regional and global connectivity measures in subjective cognitive decline depending on cerebral amyloid status. *J. Alzheimers. Dis.* 79, 493–509. doi: 10.3233/JAD-200472
- Liu, Y., Yu, C., Zhang, X., Liu, J., Duan, Y., Alexander-Bloch, A. F., et al. (2014). Impaired long distance functional connectivity and weighted network architecture in Alzheimer's disease. *Cerebral Cortex* 24, 1422–1435. doi: 10.1093/cercor/bhs410
- Machulda, M. M., Jones, D. T., Vemuri, P., Mcdade, E., Avula, R., Przybelski, S., et al. (2011). Effect of APOE  $\epsilon$ 4 status on intrinsic network connectivity in cognitively normal elderly subjects. *Arch. Neurol.* 68, 1131–1136. doi: 10.1001/archneurol.2011.108
- Mattsson, N., Insel, P. S., Nosheny, R., Tosun, D., Trojanowski, J. Q., Shaw, L. M., et al. (2014). Emerging  $\beta$ -amyloid pathology and accelerated cortical atrophy. *JAMA Neurol.* 71, 725–734. doi: 10.1001/jamaneurol.2014.446
- Mormino, E. C., Smiljic, A., Hayenga, A. O., Onami, S. H., Greicius, M. D., Rabinovici, G. D., et al. (2011). Relationships between  $\beta$ -amyloid and functional connectivity in different components of the default mode network in aging. *Cereb. Cortex* 21, 2399–2407. doi: 10.1093/cercor/bhr025
- Ng, K. K., Lo, J. C., Lim, J. K. W., Chee, M. W. L., and Zhou, J. (2016). Reduced functional segregation between the default mode network and the executive control network in healthy older adults: a longitudinal study. *Neuroimage* 133, 321–330. doi: 10.1016/j.neuroimage.2016.03.029
- Ng, K. K., Qiu, Y., Lo, J. C., Koay, E. S., Koh, W. P., Chee, M. W., et al. (2018). Functional segregation loss over time is moderated by APOE genotype in healthy elderly. *Hum. Brain Mapp.* 39, 2742–2752. doi: 10.1002/hbm.24036
- Nugent, A. C., Martinez, A., D'alfonso, A., Zarate, C. A., and Theodore, W. H. (2015). The relationship between glucose metabolism, resting-state fMRI BOLD signal, and GABAA-binding potential: a preliminary study in healthy subjects and those with temporal lobe epilepsy. *J. Cereb. Blood Flow Metab.* 35, 583–591. doi: 10.1038/jcbfm.2014.228
- Nuriel, T., Angulo, S. L., Khan, U., Ashok, A., Chen, Q., Figueroa, H. Y., et al. (2017). Neuronal hyperactivity due to loss of inhibitory tone in APOE4 mice lacking Alzheimer's disease-like pathology. *Nat. Commun.* 8, 1464. doi: 10.1038/s41467-017-01444-0
- Palmqvist, S., Schöll, M., Strandberg, O., Mattsson, N., Stomrud, E., Zetterberg, H., et al. (2017). Earliest accumulation of  $\beta$ -amyloid occurs within the default-mode network and concurrently affects brain connectivity. *Nat. Commun.* 8, 1214. doi: 10.1038/s41467-017-01150-x
- Park, J.-H. (1989). Standardization of Korean version of the mini-mental state examination (MMSE-K) for use in the elderly. Part II. Diagnostic validity. *J. Korean Neuropsychiatr. Assoc.* 28, 508–513.
- Pasquini, L., Benson, G., Grothe, M. J., Utz, L., Myers, N. E., Yakushev, I., et al. (2017). Individual correspondence of amyloid- $\beta$  and intrinsic connectivity in the posterior default mode network across stages of Alzheimer's disease. *J. Alzheimers Dis.* 58, 763–773. doi: 10.3233/JAD-170096
- Rodrigue, K. M., Kennedy, K. M., Devous, M. D. Sr., Rieck, J. R., Hebrank, A. C., Diaz-Arrastia, R., et al. (2012).  $\beta$ -Amyloid burden in healthy aging: regional distribution and cognitive consequences. *Neurology* 78, 387–395. doi: 10.1212/WNL.0b013e318245d295
- Salloway, S., Gamez, J. E., Singh, U., Sadowsky, C. H., Villena, T., Sabbagh, M. N., et al. (2017). Performance of [18F] flutemetamol amyloid imaging against the neuritic plaque component of CERAD and the current (2012) NIA-AA recommendations for the neuropathologic diagnosis of Alzheimer's disease. *Alzheimers Dement. Diagn. Assess. Dis. Monit.* 9, 25–34. doi: 10.1016/j.dadm.2017.06.001
- Schultz, A. P., Chhatwal, J. P., Hedden, T., Mormino, E. C., Hanseeuw, B. J., Sepulcre, J., et al. (2017). Phases of hyperconnectivity and hypoconnectivity in the default mode and salience networks track with amyloid and tau in clinically normal individuals. *J. Neurosci.* 37, 4323–4331. doi: 10.1523/JNEUROSCI.3263-16.2017
- Sepulcre, J., Liu, H., Talukdar, T., Martincorena, I., Yeo, B. T., and Buckner, R. L. (2010). The organization of local and distant functional connectivity in the human brain. *PLoS Comput. Biol.* 6, e1000808. doi: 10.1371/journal.pcbi.1000808
- Seto, M., Weiner, R. L., Dumitrescu, L., and Hohman, T. J. (2021). Protective genes and pathways in Alzheimer's disease: moving towards precision interventions. *Mol. Neurodegener.* 16, 1–16. doi: 10.1186/s13024-021-00452-5
- Sheline, Y. I., Morris, J. C., Snyder, A. Z., Price, J. L., Yan, Z., D'angelo, G., et al. (2010). APOE4 allele disrupts resting state fMRI connectivity in the absence of amyloid plaques or decreased CSF A $\beta$ 42. *J. Neurosci.* 30, 17035–17040. doi: 10.1523/JNEUROSCI.3987-10.2010
- Sims, R., Hill, M., and Williams, J. (2020). The multiplex model of the genetics of Alzheimer's disease. *Nat. Neurosci.* 23, 311–322. doi: 10.1038/s41593-020-0599-5
- Small, G. W., Siddarth, P., Burggren, A. C., Kepe, V., Ercoli, L. M., Miller, K. J., et al. (2009). Influence of cognitive status, age, and APOE-4 genetic risk on brain FDDNP positron-emission tomography imaging in persons without dementia. *Arch. Gen. Psychiatry* 66, 81–87. doi: 10.1001/archgenpsychiatry.2008.516
- Sojkova, J., Driscoll, I., Iacono, D., Zhou, Y., Codispoti, K. E., Kraut, M. A., et al. (2011). In vivo fibrillar beta-amyloid detected using [11C]PiB positron emission tomography and neuropathologic assessment in older adults. *Arch. Neurol.* 68, 232–240. doi: 10.1001/archneurol.2010.357
- Song, G., and Chai, W. (2018). "Collaborative learning for deep neural networks," in *Conference and Workshop on Neural Information Processing Systems*, eds S. Bengio and H. Wallach and H. Larochelle and K. Grauman and N. Cesa-Bianchi and R. Garnett (Montréal, QC), 31.
- Sorg, C., Riedel, V., Mühlau, M., Calhoun, V. D., Eichele, T., Läer, L., et al. (2007). Selective changes of resting-state networks in individuals at risk for Alzheimer's disease. *Proc. Nat. Acad. Sci.* 104, 18760–18765. doi: 10.1073/pnas.0708803104
- Sridharan, D., Levitin, D. J., and Menon, V. (2008). A critical role for the right fronto-insular cortex in switching between central-executive and default-mode networks. *Proc. Natl. Acad. Sci. U. S. A.* 105, 12569–12574. doi: 10.1073/pnas.0800005105
- Stern, Y. (2009). Cognitive reserve. *Neuropsychologia* 47, 2015–2028. doi: 10.1016/j.neuropsychologia.2009.03.004
- Stroop, J. R. (1935). Studies of interference in serial verbal reactions. *J. Exp. Psychol.* 18, 643. doi: 10.1037/h0054651
- Thurfjell, L., Lilja, J., Lundqvist, R., Buckley, C., Smith, A., Vandenberghe, R., et al. (2014). Automated quantification of 18F-flutemetamol PET activity for categorizing scans as negative or positive for brain amyloid: concordance with visual image reads. *J. Nucl. Med.* 55, 1623–1628. doi: 10.2967/jnumed.114.142109
- Tombaugh, T. N. (2004). Trail Making Test A and B: normative data stratified by age and education. *Arch. Clin. Neuropsychol.* 19, 203–214. doi: 10.1016/S0887-6177(03)00039-8
- Turner, G. R., and Spreng, R. N. (2015). Prefrontal engagement and reduced default network suppression co-occur and are dynamically coupled in older adults: the default-executive coupling hypothesis of aging. *J. Cogn. Neurosci.* 27, 2462–2476. doi: 10.1162/jocn\_a\_00869
- Villeneuve, S., Rabinovici, G. D., Cohn-Sheehy, B. I., Madison, C., Ayakta, N., Ghosh, P. M., et al. (2015). Existing Pittsburgh Compound-B positron emission tomography thresholds are too high: statistical and pathological evaluation. *Brain* 138, 2020–2033. doi: 10.1093/brain/awv112



- Wang, P., Zhou, B., Yao, H., Zhan, Y., Zhang, Z., Cui, Y., et al. (2015). Aberrant intra- and inter-network connectivity architectures in Alzheimer's disease and mild cognitive impairment. *Sci. Rep.* 5, 14824. doi: 10.1038/srep14824
- Weiler, M., Fukuda, A., Massabki, L. H. P., Lopes, T. M., Franco, A. R., Damasceno, B. P., et al. (2014). Default mode, executive function, and language functional connectivity networks are compromised in mild Alzheimer's disease. *Curr. Alzheimer Res.* 11, 274–282. doi: 10.2174/1567205011666140131114716
- Wu, X., Li, Q., Yu, X., Chen, K., Fleisher, A. S., Guo, X., et al. (2016). A triple network connectivity study of large-scale brain systems in cognitively normal APOE4 carriers. *Front. Aging Neurosci.* 8, 231. doi: 10.3389/fnagi.2016.00231
- Yan, C., and Zang, Y. (2010). DPARSF: a MATLAB toolbox for "pipeline" data analysis of resting-state fMRI. *Front. Syst. Neurosci.* 4, 13. doi: 10.3389/fnsys.2010.00013
- Yi, D., Lee, D. Y., Sohn, B. K., Choe, Y. M., Seo, E. H., Byun, M. S., et al. (2014). Beta-amyloid associated differential effects of APOE  $\epsilon$ 4 on brain metabolism in cognitively normal elderly. *Am. J. Geriatr. Psychiatry* 22, 961–970. doi: 10.1016/j.jagp.2013.12.173
- Zang, Y., Jiang, T., Lu, Y., He, Y., and Tian, L. (2004). Regional homogeneity approach to fMRI data analysis. *Neuroimage* 22, 394–400. doi: 10.1016/j.neuroimage.2003.12.030
- Zhu, D. C., Majumdar, S., Korolev, I. O., Berger, K. L., and Bozoki, A. C. (2013). Alzheimer's disease and amnesic mild cognitive impairment weaken connections within the default-mode network: a multi-modal imaging study. *J. Alzheimers Dis.* 34, 969–984. doi: 10.3233/JAD-121879
- Zott, B., Simon, M. M., Hong, W., Unger, F., Chen-Engerer, H.-J., Frosch, M. P., et al. (2019). A vicious cycle of  $\beta$  amyloid-dependent neuronal hyperactivation. *Science* 365, 559–565. doi: 10.1126/science.aay0198
- Conflict of Interest:** The authors declare that the research was conducted in the absence of any commercial or financial relationships that could be construed as a potential conflict of interest.
- Publisher's Note:** All claims expressed in this article are solely those of the authors and do not necessarily represent those of their affiliated organizations, or those of the publisher, the editors and the reviewers. Any product that may be evaluated in this article, or claim that may be made by its manufacturer, is not guaranteed or endorsed by the publisher.
- Copyright © 2022 Kang, Wang, Um, Kim, Lee and Lim. This is an open-access article distributed under the terms of the Creative Commons Attribution License (CC BY). The use, distribution or reproduction in other forums is permitted, provided the original author(s) and the copyright owner(s) are credited and that the original publication in this journal is cited, in accordance with accepted academic practice. No use, distribution or reproduction is permitted which does not comply with these terms.